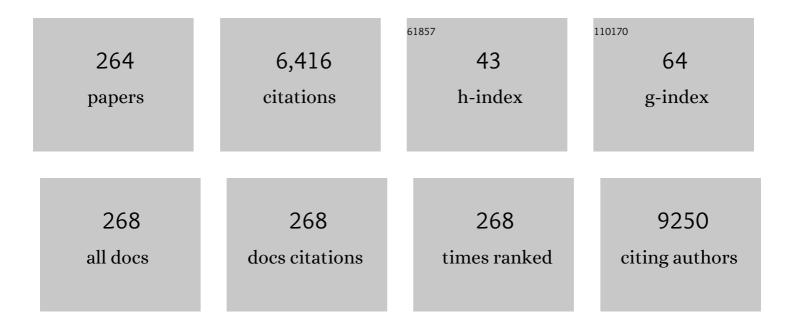
Marco De Spirito

List of Publications by Year in descending order

Source: https://exaly.com/author-pdf/9221272/publications.pdf Version: 2024-02-01



#	Article	IF	CITATIONS
1	Label-free spectroscopic characterization of exosomes reveals cancer cell differentiation. Analytica Chimica Acta, 2022, 1192, 339359.	2.6	12
2	Post mortem computed tomography meets radiomics: a case series on fractal analysis of post mortem changes in the brain. International Journal of Legal Medicine, 2022, 136, 719-727.	1.2	3
3	INSIDIA 2.0 High-Throughput Analysis of 3D Cancer Models: Multiparametric Quantification of Graphene Quantum Dots Photothermal Therapy for Clioblastoma and Pancreatic Cancer. International Journal of Molecular Sciences, 2022, 23, 3217.	1.8	9
4	Personalized Self-Monitoring of Energy Balance through Integration in a Web-Application of Dietary, Anthropometric, and Physical Activity Data. Journal of Personalized Medicine, 2022, 12, 568.	1.1	10
5	Automated detection and classification of tumor histotypes on dynamic PET imaging data through machine-learning driven voxel classification. Computers in Biology and Medicine, 2022, 145, 105423.	3.9	11
6	3D-printed graphene polylactic acid devices resistant to SARS-CoV-2: Sunlight-mediated sterilization of additive manufactured objects. Carbon, 2022, 194, 34-41.	5.4	14
7	Opportunities Offered by Graphene Nanoparticles for MicroRNAs Delivery for Amyotrophic Lateral Sclerosis Treatment. Materials, 2022, 15, 126.	1.3	5
8	Investigation of DHA-Induced Regulation of Redox Homeostasis in Retinal Pigment Epithelium Cells through the Combination of Metabolic Imaging and Molecular Biology. Antioxidants, 2022, 11, 1072.	2.2	8
9	Unsupervised Clustering of Heartbeat Dynamics Allows for Real Time and Personalized Improvement in Cardiovascular Fitness. Sensors, 2022, 22, 3974.	2.1	7
10	Machine Learning-Assisted FTIR Analysis of Circulating Extracellular Vesicles for Cancer Liquid Biopsy. Journal of Personalized Medicine, 2022, 12, 949.	1.1	17
11	Enoxaparin Increases D6 Receptor Expression and Restores Cytoskeleton Organization in Trophoblast Cells from Preeclampsia. Cells, 2022, 11, 2036.	1.8	0
12	Erythrocyte membrane fluidity as a marker of diabetic retinopathy in type 1 diabetes mellitus. European Journal of Clinical Investigation, 2021, 51, e13455.	1.7	18
13	A field strength independent MR radiomics model to predict pathological complete response in locally advanced rectal cancer. Radiologia Medica, 2021, 126, 421-429.	4.7	67
14	Nuclear Localization of PTTG1 Promotes Migration and Invasion of Seminoma Tumor through Activation of MMP-2. Cancers, 2021, 13, 212.	1.7	10
15	Evaluation of a generalized knowledge-based planning performance for VMAT irradiation of breast and locoregional lymph nodes—Internal mammary and/or supraclavicular regions. PLoS ONE, 2021, 16, e0245305.	1.1	10
16	Functionalized Graphene Quantum Dots Modulate Malignancy of Glioblastoma Multiforme by Downregulating Neurospheres Formation. Journal of Carbon Research, 2021, 7, 4.	1.4	4
17	Label-free metabolic clustering through unsupervised pixel classification of multiparametric fluorescent images. Analytica Chimica Acta, 2021, 1148, 238173.	2.6	13
18	Visco-Hyperelastic Characterization of the Equine Immature Zona Pellucida. Materials, 2021, 14, 1223.	1.3	6

#	Article	IF	CITATIONS
19	Investigation of the Membrane Fluidity Regulation of Fatty Acid Intracellular Distribution by Fluorescence Lifetime Imaging of Novel Polarity Sensitive Fluorescent Derivatives. International Journal of Molecular Sciences, 2021, 22, 3106.	1.8	13
20	Face masks and nanotechnology: Keep the blue side up. Nano Today, 2021, 37, 101077.	6.2	83
21	Recent Advances in the Label-Free Characterization of Exosomes for Cancer Liquid Biopsy: From Scattering and Spectroscopy to Nanoindentation and Nanodevices. Nanomaterials, 2021, 11, 1476.	1.9	25
22	Graphene nanoplatelet and graphene oxide functionalization of face mask materials inhibits infectivity of trapped SARS-CoV-2. IScience, 2021, 24, 102788.	1.9	59
23	Attenuated total reflection-Fourier transform infrared spectroscopy (ATR-FTIR) detection as a rapid and convenient screening test for cystinuria. Clinica Chimica Acta, 2021, 518, 128-133.	0.5	6
24	Nanofeatures of orthopedic implant surfaces. Nanomedicine, 2021, 16, 1733-1736.	1.7	3
25	In situ N-acetylcysteine release from polyvinyl alcohol film for moisture-activated food packaging. Food Packaging and Shelf Life, 2021, 29, 100694.	3.3	3
26	Estimation of the time of death by measuring the variation of lateral cerebral ventricle volume and cerebrospinal fluid radiodensity using postmortem computed tomography. International Journal of Legal Medicine, 2021, 135, 2615-2623.	1.2	8
27	Laser-Mediated antibacterial effects of Few- and Multi-Layer Ti3C2Tx MXenes. Applied Surface Science, 2021, 567, 150795.	3.1	48
28	Recurrence quantification analysis of heart rate variability to detect both ventilatory thresholds. PLoS ONE, 2021, 16, e0249504.	1.1	13
29	RadiomiK phantom to test the robustness of CT radiomic features. Physica Medica, 2021, 92, S29.	0.4	0
30	Serum immunoglobulin free light chain levels in systemic autoimmune rheumatic diseases. Clinical and Experimental Immunology, 2020, 199, 163-171.	1.1	22
31	On the accuracy of bulk synthetic CT for MR-guided online adaptive radiotherapy. Radiologia Medica, 2020, 125, 157-164.	4.7	24
32	Fourier Transform Infrared Spectroscopy as a useful tool for the automated classification of cancer cell-derived exosomes obtained under different culture conditions. Analytica Chimica Acta, 2020, 1140, 219-227.	2.6	21
33	External Validation of Early Regression Index (ERITCP) as Predictor of Pathologic Complete Response in Rectal Cancer Using Magnetic Resonance-Guided Radiation Therapy. International Journal of Radiation Oncology Biology Physics, 2020, 108, 1347-1356.	0.4	34
34	Graphene Oxide-Linezolid Combination as Potential New Anti-Tuberculosis Treatment. Nanomaterials, 2020, 10, 1431.	1.9	20
35	An evaluation of the objectivity and reproducibility of shear wave elastography in estimating the post-mortem interval: a tissue biomechanical perspective. International Journal of Legal Medicine, 2020, 134, 1939-1948.	1.2	11
36	Searching for the Mechanical Fingerprint of Pre-diabetes in T1DM: A Case Report Study. Frontiers in Bioengineering and Biotechnology, 2020, 8, 569978.	2.0	5

#	Article	IF	CITATIONS
37	Enhanced Chemotherapy for Glioblastoma Multiforme Mediated by Functionalized Graphene Quantum Dots. Materials, 2020, 13, 4139.	1.3	28
38	Graphene Quantum Dots' Surface Chemistry Modulates the Sensitivity of Glioblastoma Cells to Chemotherapeutics. International Journal of Molecular Sciences, 2020, 21, 6301.	1.8	32
39	Living optical random neural network with three dimensional tumor spheroids for cancer morphodynamics. Communications Physics, 2020, 3, .	2.0	14
40	Erythrocyte viscoelastic recovery after liver transplantation in a cirrhotic patient affected by spur cell anaemia. Journal of Microscopy, 2020, 280, 287-296.	0.8	6
41	Characterization of an inorganic scintillator for smallâ€field dosimetry in MRâ€guided radiotherapy. Journal of Applied Clinical Medical Physics, 2020, 21, 244-251.	0.8	10
42	Unravelling the Potential of Graphene Quantum Dots in Biomedicine and Neuroscience. International Journal of Molecular Sciences, 2020, 21, 3712.	1.8	77
43	3D Graphene Scaffolds for Skeletal Muscle Regeneration: Future Perspectives. Frontiers in Bioengineering and Biotechnology, 2020, 8, 383.	2.0	28
44	Reliability of ITV approach to varying treatment fraction time: a retrospective analysis based on 2D cine MR images. Radiation Oncology, 2020, 15, 152.	1.2	13
45	A time-dependent study of nano-mechanical and ultrastructural properties of internal limiting membrane under ocriplasmin treatment. Journal of the Mechanical Behavior of Biomedical Materials, 2020, 110, 103853.	1.5	8
46	Graphene-based scaffolds for tissue engineering and photothermal therapy. Nanomedicine, 2020, 15, 1411-1417.	1.7	32
47	Graphene Oxide Nano-Concentrators Selectively Modulate RNA Trapping According to Metal Cations in Solution. Frontiers in Bioengineering and Biotechnology, 2020, 8, 421.	2.0	8
48	3D-printed graphene for bone reconstruction. 2D Materials, 2020, 7, 022004.	2.0	27
49	Altered mitochondrial function in cells carrying a premutation or unmethylated full mutation of the FMR1 gene. Human Genetics, 2020, 139, 227-245.	1.8	16
50	Recurrence quantification analysis of heart rate variability during continuous incremental exercise test in obese subjects. Chaos, 2020, 30, 033135.	1.0	17
51	Machine-learning assisted confocal imaging of intracellular sites of triglycerides and cholesteryl esters formation and storage. Analytica Chimica Acta, 2020, 1121, 57-66.	2.6	17
52	Unsupervised clustering of multiparametric fluorescent images extends the spectrum of detectable cell membrane phases with sub-micrometric resolution. Biomedical Optics Express, 2020, 11, 5728.	1.5	10
53	On the Role of Human Umbilical Cord Biomechanics. Conference Proceedings of the Society for Experimental Mechanics, 2020, , 81-86.	0.3	0
54	PH-0715: External validation of ERITCP as response predictor in rectal cancer using MR-guided Radiotherapy. Radiotherapy and Oncology, 2020, 152, S404-S405.	0.3	0

#	Article	IF	CITATIONS
55	PO-1536: RadiomiK: a phantom to test repeatability and reproducibility of CT-derived Radiomic Features. Radiotherapy and Oncology, 2020, 152, S830-S831.	0.3	1
56	PO-1613: Reliability of ITV approach to varying treatment fraction time: considerations based on 2D cine MRI. Radiotherapy and Oncology, 2020, 152, S878-S879.	0.3	0
57	PO-1474: Automated VMAT-SBRT treatment planning for complex spinal metastases: a dosimetric analysis. Radiotherapy and Oncology, 2020, 152, S791.	0.3	Ο
58	PO-1503: Evaluation of a generalized knowledge-based planning for VMAT irradiation of breast and lymph nodes. Radiotherapy and Oncology, 2020, 152, S810-S811.	0.3	0
59	PO-1329: Characterisation of a scintillator for small fields and in-vivo dosimetry in MR guided Radiotherapy. Radiotherapy and Oncology, 2020, 152, S701-S702.	0.3	0
60	Nanomechanical mapping helps explain differences in outcomes of eye microsurgery: A comparative study of macular pathologies. PLoS ONE, 2019, 14, e0220571.	1.1	16
61	The biomechanics of the umbilical cord Wharton Jelly: Roles in hemodynamic proficiency and resistance to compression. Journal of the Mechanical Behavior of Biomedical Materials, 2019, 100, 103377.	1.5	8
62	Efficient Spatial Sampling for AFM-Based Cancer Diagnostics: A Comparison between Neural Networks and Conventional Data Analysis. Condensed Matter, 2019, 4, 58.	0.8	13
63	Red blood cells membrane micropolarity as a novel diagnostic indicator of type 1 and type 2 diabetes. Analytica Chimica Acta: X, 2019, 3, 100030.	2.8	10
64	EP-2012 MR-guided online adaptive radiotherapy for pancreatic cancer: where are we and where are we going?. Radiotherapy and Oncology, 2019, 133, S1102-S1103.	0.3	0
65	Dynamic structural determinants underlie the neurotoxicity of the N-terminal tau 26-44 peptide in Alzheimer's disease and other human tauopathies. International Journal of Biological Macromolecules, 2019, 141, 278-289.	3.6	16
66	Evaluation of a simplified optimizer for MRâ€guided adaptive RT in case of pancreatic cancer. Journal of Applied Clinical Medical Physics, 2019, 20, 20-30.	0.8	8
67	PV-0310 A field strength independent MR radiomics model for pathological complete response in rectal cancer. Radiotherapy and Oncology, 2019, 133, S158-S159.	0.3	Ο
68	EP-1468 Radiomics versus volume reduction for rectal cancer response prediction in hybrid MR guided RT. Radiotherapy and Oncology, 2019, 133, S796-S797.	0.3	0
69	EP-2011 Dose calculation accuracy of using tailored synthetic CT for MR-guided online adaptive radiotherapy. Radiotherapy and Oncology, 2019, 133, S1101-S1102.	0.3	Ο
70	Carbon nanomaterials: a new way against tuberculosis. Expert Review of Medical Devices, 2019, 16, 863-875.	1.4	16
71	Graphene oxide touches blood: <i>in vivo</i> interactions of bio-coronated 2D materials. Nanoscale Horizons, 2019, 4, 273-290.	4.1	97
72	Imaging of Lipid Metabolism through a Phasor Analysis of Membrane Micropolarity. Biophysical Journal, 2019, 116, 81a.	0.2	0

#	Article	IF	CITATIONS
73	A novel method for post-mortem interval estimation based on tissue nano-mechanics. International Journal of Legal Medicine, 2019, 133, 1133-1139.	1.2	20
74	Biocompatible <i>N</i> -acetyl cysteine reduces graphene oxide and persists at the surface as a green radical scavenger. Chemical Communications, 2019, 55, 4186-4189.	2.2	25
75	Graphene oxide prevents mycobacteria entry into macrophages through extracellular entrapment. Nanoscale Advances, 2019, 1, 1421-1431.	2.2	28
76	Hexadecenoic Fatty Acid Positional Isomers and De Novo PUFA Synthesis in Colon Cancer Cells. International Journal of Molecular Sciences, 2019, 20, 832.	1.8	35
77	Low-Intensity Ultrasound Induces Thermodynamic Phase Separation of Cell Membranes through a Nucleation–Condensation Process. Ultrasound in Medicine and Biology, 2019, 45, 1143-1150.	0.7	12
78	Optical Neural Network by Disordered Tumor Spheroids. , 2019, , .		2
79	A protein chimera selfâ€assembling unit for drug delivery. Biotechnology Progress, 2019, 35, e2769.	1.3	1
80	Delta radiomics for rectal cancer response prediction with hybrid 0.35ÂT magnetic resonance-guided radiotherapy (MRgRT): a hypothesis-generating study for an innovative personalized medicine approach. Radiologia Medica, 2019, 124, 145-153.	4.7	112
81	Inhibition of Transglutaminase 2 as a Potential Host-Directed Therapy Against Mycobacterium tuberculosis. Frontiers in Immunology, 2019, 10, 3042.	2.2	13
82	Optical neural network for cancer morphodynamics sensing. , 2019, , .		1
83	Curcumin-loaded graphene oxide flakes as an effective antibacterial system against methicillin-resistant <i>Staphylococcus aureus</i> . Interface Focus, 2018, 8, 20170059.	1.5	61
84	Real time quantitative analysis of lipid storage and lipolysis pathways by confocal spectral imaging of intracellular micropolarity. Biochimica Et Biophysica Acta - Molecular and Cell Biology of Lipids, 2018, 1863, 783-793.	1.2	18
85	Antibacterial Properties of Curcumin Loaded Graphene Oxide Flakes. Biophysical Journal, 2018, 114, 362a.	0.2	3
86	Graphene Oxide Laser Printing for Controlled STEM Cells Differentiation and Antibacterial Effects. Biophysical Journal, 2018, 114, 362a-363a.	0.2	0
87	Systemic profiling of ectopic fat deposits in the reproductive tract of dairy cows. Theriogenology, 2018, 114, 46-53.	0.9	8
88	Neural Network Approach for the Analysis of AFM Force-Distance Curves for Brain Cancer Diagnosis. Biophysical Journal, 2018, 114, 353a.	0.2	3
89	Fractal-based radiomic approach to predict complete pathological response after chemo-radiotherapy in rectal cancer. Radiologia Medica, 2018, 123, 286-295.	4.7	91
90	Reduction and shaping of graphene-oxide by laser-printing for controlled bone tissue regeneration and bacterial killing. 2D Materials, 2018, 5, 015027.	2.0	32

#	Article	IF	CITATIONS
91	Transglutaminase type 2 plays a key role in the pathogenesis of <i>Mycobacterium tuberculosis</i> infection. Journal of Internal Medicine, 2018, 283, 303-313.	2.7	23
92	146. Comparing group based and patient specific cone-beam CT intensity correction methods for VMAT dose recalculations. Physica Medica, 2018, 56, 155.	0.4	0
93	Delta Radiomics Analysis for Hybrid MR-RT Imaging in Rectal Cancer for Response Prediction: A Hypothesis Generating Study. International Journal of Radiation Oncology Biology Physics, 2018, 102, e1.	0.4	0
94	Graphene oxide coatings prevent <i>Candida albicans</i> biofilm formation with a controlled release of curcumin-loaded nanocomposites. Nanomedicine, 2018, 13, 2867-2879.	1.7	57
95	Graphene Oxide Induced Osteogenesis Quantification by In-Situ 2D-Fluorescence Spectroscopy. International Journal of Molecular Sciences, 2018, 19, 3336.	1.8	12
96	Quantitative imaging of membrane micropolarity in living cells and tissues by spectral phasors analysis. MethodsX, 2018, 5, 1399-1412.	0.7	8
97	PE_PGRS3 of <i>Mycobacterium tuberculosis</i> is specifically expressed at low phosphate concentration, and its arginine-rich C-terminal domain mediates adhesion and persistence in host tissues when expressed in <i>Mycobacterium smegmatis</i> . Cellular Microbiology, 2018, 20, e12952.	1.1	24
98	A decision support system for type 1 diabetes mellitus diagnostics based on dual channel analysis of red blood cell membrane fluidity. Computer Methods and Programs in Biomedicine, 2018, 162, 263-271.	2.6	30
99	OC-0186: Real-time long-term multi-object tracking on cineMR using a tracking-learning-detection framework. Radiotherapy and Oncology, 2018, 127, S99-S100.	0.3	1
100	OC-0300: Linac MRI guided SBRT treatment in pancreatic cancer: dosimetric evaluation of a new technology. Radiotherapy and Oncology, 2018, 127, S156-S157.	0.3	1
101	Nanoscale mechanics of brain abscess: An atomic force microscopy study. Micron, 2018, 113, 34-40.	1.1	19
102	EP-1821: Evaluation of dose calculation accuracy at lung-tissue interface in presence of 0.35T magnetic field. Radiotherapy and Oncology, 2018, 127, S981-S982.	0.3	0
103	Hybrid Tri-Co-60 MRI radiotherapy for locally advanced rectal cancer: An in silico evaluation. Technical Innovations and Patient Support in Radiation Oncology, 2018, 6, 5-10.	0.6	12
104	Predicting tumour motion during the whole radiotherapy treatment: a systematic approach for thoracic and abdominal lesions based on real time MR. Radiotherapy and Oncology, 2018, 129, 456-462.	0.3	56
105	Experimental evaluation of the impact of low tesla transverse magnetic field on dose distribution in presence of tissue interfaces. Physica Medica, 2018, 53, 80-85.	0.4	22
106	Nonlinear optics, optomechanics, and antibacterial coating by graphene oxide. , 2017, , .		0
107	Bacteria Meet Graphene: Modulation of Graphene Oxide Nanosheet Interaction with Human Pathogens for Effective Antimicrobial Therapy. ACS Biomaterials Science and Engineering, 2017, 3, 619-627.	2.6	115
108	α-Dystroglycan hypoglycosylation affects cell migration by influencing β-dystroglycan membrane clustering and filopodia length: A multiscale confocal microscopy analysis. Biochimica Et Biophysica Acta - Molecular Basis of Disease, 2017, 1863, 2182-2191.	1.8	12

#	Article	IF	CITATIONS
109	Differentiation Affects the Release of Exosomes from Colon Cancer Cells and Their Ability to Modulate the Behavior of Recipient Cells. American Journal of Pathology, 2017, 187, 1633-1647.	1.9	42
110	Graphene-Oxide Gel as Biomimetic Antimicrobial Cloak. Biophysical Journal, 2017, 112, 589a.	0.2	0
111	Modulation of Graphene Oxide Probiotic and Antibiotic Activity by Critical Coagulation Concentration. Biophysical Journal, 2017, 112, 156a-157a.	0.2	0
112	The graphene oxide contradictory effects against human pathogens. Nanotechnology, 2017, 28, 152001.	1.3	84
113	Nanoindentation characterisation of human colorectal cancer cells considering cell geometry, surface roughness and hyperelastic constitutive behaviour. Nanotechnology, 2017, 28, 045703.	1.3	18
114	EPID-based in vivo dosimetry for stereotactic body radiotherapy of non-small cell lung tumors: Initial clinical experience. Physica Medica, 2017, 42, 157-161.	0.4	15
115	Development and Validation of New Radiomic Features Based on Fractal Analysis. International Journal of Radiation Oncology Biology Physics, 2017, 99, S83.	0.4	0
116	Towards Tumor Margins Reduction: Tracking Accuracy Evaluation of an MRI-RT System. International Journal of Radiation Oncology Biology Physics, 2017, 99, S124-S125.	0.4	0
117	A fully-automated neural network analysis of AFM force-distance curves for cancer tissue diagnosis. Applied Physics Letters, 2017, 111, .	1.5	47
118	EP-1683: Fractals in Radiomics: implementation of new features based on fractal analysis. Radiotherapy and Oncology, 2017, 123, S918.	0.3	0
119	Different effects of matrix degrading enzymes towards biofilms formed by E. faecalis and E. faecium clinical isolates. Colloids and Surfaces B: Biointerfaces, 2017, 158, 349-355.	2.5	31
120	INSIDIA: A FIJI Macro Delivering Highâ€Throughput and Highâ€Content Spheroid Invasion Analysis. Biotechnology Journal, 2017, 12, 1700140.	1.8	32
121	Nano-Mechanical Response of Red Blood Cells. Conference Proceedings of the Society for Experimental Mechanics, 2017, , 11-16.	0.3	4
122	Viscohyperelastic Calibration in Mechanical Characterization of Soft Matter. Conference Proceedings of the Society for Experimental Mechanics, 2017, , 33-37.	0.3	0
123	Mechanic Adaptability of Metastatic Cells in Colon Cancer. Conference Proceedings of the Society for Experimental Mechanics, 2017, , 1-9.	0.3	0
124	PUB001 Epid-Based in Vivo Dosimetry for Accurate Delivery of Lung Stereotactic Radiotherapy Using Breath-Hold Segmented VMAT. Journal of Thoracic Oncology, 2017, 12, S2365.	0.5	0
125	Phase separation of the plasma membrane in human red blood cells as a potential tool for diagnosis and progression monitoring of type 1 diabetes mellitus. PLoS ONE, 2017, 12, e0184109.	1.1	23

126 Optical supercavitation in graphene-oxide hydrogel for antimicrobial cloaks. , 2017, , .

0

#	Article	IF	CITATIONS
127	Changes in cellular mechanical properties during onset or progression of colorectal cancer. World Journal of Gastroenterology, 2016, 22, 7203.	1.4	55
128	Estradiol protective role in atherogenesis through LDL structure modification. Journal Physics D: Applied Physics, 2016, 49, 285402.	1.3	2
129	Biomimetic antimicrobial cloak by graphene-oxide agar hydrogel. Scientific Reports, 2016, 6, 12.	1.6	143
130	Quantitative Analysis of Autophagic Flux by Ratiometric pH-Imaging of Autophagic Intermediates. Biophysical Journal, 2016, 110, 596a.	0.2	0
131	Role of AL, FE, CU in the Alterations of Mechanical Properties of Cortical Neurons Probed by Atomic Force Microscopy. Biophysical Journal, 2016, 110, 148a.	0.2	Ο
132	Nanoscale Mapping of the Biomechanical Behavior in Healthy and Pathological Erythrocytes. Biophysical Journal, 2016, 110, 308a.	0.2	0
133	Imaging Reactive Oxygen Species-Induced Modifications in Living Systems. Antioxidants and Redox Signaling, 2016, 24, 939-958.	2.5	43
134	Fatty acid-related modulations of membrane fluidity in cells: detection and implications. Free Radical Research, 2016, 50, S40-S50.	1.5	112
135	The future development of bacteria fighting medical devices: the role of graphene oxide. Expert Review of Medical Devices, 2016, 13, 1013-1019.	1.4	83
136	<i>In vitro</i> effect of clarithromycin and alginate lyase against <i>helicobacter pylori</i> biofilm. Biotechnology Progress, 2016, 32, 1584-1591.	1.3	25
137	Nano-mechanical signature of brain tumours. Nanoscale, 2016, 8, 19629-19643.	2.8	75
138	Debris of carbon-fibers originated from a CFRP (pEEK) wrist-plate triggered a destruent synovitis in human. Journal of Materials Science: Materials in Medicine, 2016, 27, 50.	1.7	12
139	Towards a "Green―Antimicrobial Therapy: Study of Graphene Nanosheets Interaction with Human Pathogens. Biophysical Journal, 2016, 110, 530a.	0.2	0
140	Plasma Protein Corona Reduces the Haemolytic Activity of the Graphene Oxide Nano and Micro Flakes. Biophysical Journal, 2016, 110, 167a.	0.2	1
141	Recent advances in superhydrophobic surfaces and their relevance to biology and medicine. Bioinspiration and Biomimetics, 2016, 11, 011001.	1.5	44
142	A Deeper Look Into Immature Porcine Zona Pellucida Visco-hyperelasticity. Conference Proceedings of the Society for Experimental Mechanics, 2016, , 85-89.	0.3	1
143	Placental Chemokine Receptor D6 Is Functionally Impaired in Pre-Eclampsia. PLoS ONE, 2016, 11, e0164747.	1.1	8
144	Modulation of the α-Crystallin Chaperon Activity Induced by Changes in the Exposed Surface. Biophysical Journal, 2015, 108, 53a.	0.2	0

#	Article	IF	CITATIONS
145	Human IgG Antinuclear Antibodies Induce Pregnancy Loss in Mice by Increasing Immune Complex Deposition in Placental Tissue: <i>In Vivo</i> Study. American Journal of Reproductive Immunology, 2015, 74, 542-552.	1.2	29
146	VP6-SUMO Self-Assembly as Nanocarriers for Gastrointestinal Delivery. Journal of Nanomaterials, 2015, 2015, 1-7.	1.5	7
147	Effect of Alginate Lyase on Biofilm-Grown <i>Helicobacter pylori</i> Probed by Atomic Force Microscopy. International Journal of Polymer Science, 2015, 2015, 1-9.	1.2	288
148	ER stress induced by the OCH1 mutation triggers changes in lipid homeostasis in Kluyveromyces lactis. Research in Microbiology, 2015, 166, 84-92.	1.0	6
149	Controlling DNA Bundle Size and Spatial Arrangement in Self-assembled Arrays on Superhydrophobic Surface. Nano-Micro Letters, 2015, 7, 146-151.	14.4	9
150	An integrated superhydrophobic-plasmonic biosensor for mid-infrared protein detection at the femtomole level. Physical Chemistry Chemical Physics, 2015, 17, 21337-21342.	1.3	27
151	Effect of AFM probe geometry on visco-hyperelastic characterization of soft materials. Nanotechnology, 2015, 26, 325701.	1.3	23
152	Mechanical and structural comparison between primary tumor and lymph node metastasis cells in colorectal cancer. Soft Matter, 2015, 11, 5719-5726.	1.2	72
153	Stearoyl-CoA desaturase 1 and paracrine diffusible signals have a major role in the promotion of breast cancer cell migration induced by cancer-associated fibroblasts. British Journal of Cancer, 2015, 112, 1675-1686.	2.9	36
154	In vitro effect of temperature on the conformational structure and collagen binding of SdrF, a Staphylococcus epidermidis adhesin. Applied Microbiology and Biotechnology, 2015, 99, 5593-5603.	1.7	4
155	Plasma protein corona reduces the haemolytic activity of graphene oxide nano and micro flakes. RSC Advances, 2015, 5, 81638-81641.	1.7	48
156	Quantitative analysis of autophagic flux by confocal pH-imaging of autophagic intermediates. Autophagy, 2015, 11, 1905-1916.	4.3	68
157	Mapping viscoelastic properties of healthy and pathological red blood cells at the nanoscale level. Nanoscale, 2015, 7, 17030-17037.	2.8	86
158	A Preliminary Investigation on the Mechanical Behavior of Umbilical Cord With Moiré Techniques. Conference Proceedings of the Society for Experimental Mechanics, 2015, , 47-52.	0.3	0
159	Study on the Visco-Hyperelastic Behavior of the Zona Pellucida. Conference Proceedings of the Society for Experimental Mechanics, 2015, , 53-62.	0.3	1
160	Impact of Protein Domains on PE_PGRS30 Polar Localization in Mycobacteria. PLoS ONE, 2014, 9, e112482.	1.1	29
161	Novel fluorescent security marker. Part II: application of novel 6-alkoxy-2-amino-3,5-pyridinedicarbonitrile nanoparticles in safety paper. RSC Advances, 2014, 4, 59614-59625.	1.7	12
162	Biomechanical investigation of colorectal cancer cells. Applied Physics Letters, 2014, 105, 123701.	1.5	34

#	Article	IF	CITATIONS
163	A hybrid characterization framework to determine the visco-hyperelastic properties of a porcine zona pellucida. Interface Focus, 2014, 4, 20130066.	1.5	33
164	Gelatin tannate ameliorates acute colitis in mice by reinforcing mucus layer and modulating gut microbiota composition: Emerging role for â€~gut barrier protectors' in IBD?. United European Gastroenterology Journal, 2014, 2, 113-122.	1.6	31
165	OC.12.1 MORPHOLOGICAL FEATURES OF ENDOTHELIAL CELLS OF ENDOMETRIUM BEFORE AND AFTER INCUBATION WITH ANTI-TRANSGLUTAMINASE ANTIBODIES IN BOTH HEALTHY AND CELIAC WOMEN. Digestive and Liver Disease, 2014, 46, S28.	0.4	Ο
166	IRIDE: Interdisciplinary research infrastructure based on dual electron linacs and lasers. Nuclear Instruments and Methods in Physics Research, Section A: Accelerators, Spectrometers, Detectors and Associated Equipment, 2014, 740, 138-146.	0.7	9
167	Dynamic light scattering for the characterization and counting of extracellular vesicles: a powerful noninvasive tool. Journal of Nanoparticle Research, 2014, 16, 1.	0.8	88
168	Controlling the Cassie-to-Wenzel Transition: an Easy Route towards the Realization of Tridimensional Arrays of Biological Objects. Nano-Micro Letters, 2014, 6, 280-286.	14.4	14
169	Celiac disease and reproductive disorders: meta-analysis of epidemiologic associations and potential pathogenic mechanisms. Human Reproduction Update, 2014, 20, 582-593.	5.2	123
170	Assessing the feasibility of volumetric-modulated arc therapy using simultaneous integrated boost (SIB-VMAT): An analysis for complex head-neck, high-risk prostate and rectal cancer cases. Medical Dosimetry, 2014, 39, 108-116.	0.4	23
171	Time evolution of noise induced oxidation in outer hair cells: Role of NAD(P)H and plasma membrane fluidity. Biochimica Et Biophysica Acta - General Subjects, 2014, 1840, 2192-2202.	1.1	45
172	Quantitative Assessment of the Relationship Between Cellular Morphodynamics and Signaling Events by Stochastic Analysis of Fluorescent Images. Microscopy and Microanalysis, 2014, 20, 1198-1207.	0.2	3
173	Misfolding of Apoprotein B-100, LDL Aggregation and 17-β -estradiol in Atherogenesis. Current Medicinal Chemistry, 2014, 21, 2276-2283.	1.2	10
174	Controlling the Cassie-to-Wenzel Transition: an Easy Route towards the Realization of Tridimensional Arrays of Biological Objects. Nano-Micro Letters, 2014, 6, 280.	14.4	1
175	αâ€Crystallin Modulates its Chaperone Activity by Varying the Exposed Surface. ChemBioChem, 2013, 14, 2362-2370.	1.3	11
176	Applicator-guided volumetric-modulated arc therapy for low-risk endometrial cancer. Medical Dosimetry, 2013, 38, 5-11.	0.4	12
177	Self-assembling of large ordered DNA arrays using superhydrophobic patterned surfaces. Nanotechnology, 2013, 24, 495302.	1.3	30
178	A fast and quantitative evaluation of the Aspergillus fumigatus biofilm adhesion properties by means of digital pulsed force mode. Applied Surface Science, 2013, 279, 409-415.	3.1	10
179	Mycobacterium tuberculosis may escape helper T cell recognition by infecting human fibroblasts. Human Immunology, 2013, 74, 722-729.	1.2	18
180	Potential New Mechanisms of Placental Damage in Celiac Disease: Anti-Transglutaminase Antibodies Impair Human Endometrial Angiogenesis1. Biology of Reproduction, 2013, 89, 88.	1.2	32

#	Article	IF	CITATIONS
181	Viscous forces are predominant in the zona pellucida mechanical resistance. Applied Physics Letters, 2013, 102, .	1.5	22
182	The typeÂ2B p.R1306W natural mutation of von Willebrand factor dramatically enhances the multimer sensitivity to shear stress. Journal of Thrombosis and Haemostasis, 2013, 11, 1688-1698.	1.9	15
183	Effect of the residual stress on soft sample nanoindentation. Applied Physics Letters, 2013, 102, 133704.	1.5	21
184	In VitroInteraction between Alginate Lyase and Amphotericin B against Aspergillus fumigatus Biofilm Determined by Different Methods. Antimicrobial Agents and Chemotherapy, 2013, 57, 1275-1282.	1.4	45
185	Leuprorelin Acetate Long-Lasting Effects on GnRH Receptors of Prostate Cancer Cells: An Atomic Force Microscopy Study of Agonist/Receptor Interaction. PLoS ONE, 2013, 8, e52530.	1.1	14
186	Quality of Life and Toxicity of Stereotactic Radiotherapy in Pancreatic Tumors: A Case Series. Cancer Investigation, 2012, 30, 149-155.	0.6	23
187	Nanoscale characterization of the biomechanical hardening of bovine zona pellucida. Journal of the Royal Society Interface, 2012, 9, 2871-2882.	1.5	55
188	Impact of electronegative low-density lipoprotein on angiographic coronary atherosclerotic burden. Atherosclerosis, 2012, 223, 166-170.	0.4	13
189	Detection of Biofilm-Grown <i>Aspergillus fumigatus</i> by Means of Atomic Force Spectroscopy: Ultrastructural Effects of Alginate Lyase. Microscopy and Microanalysis, 2012, 18, 1088-1094.	0.2	23
190	The Thermal Structural Transition of Alpha-Crystallin Modulates Subunit Interactions and Increases Protein Solubility. PLoS ONE, 2012, 7, e30705.	1.1	5
191	Whole-Depth Change in Bovine Zona Pellucida Biomechanics after Fertilization: How Relevant in Hindering Polyspermy?. PLoS ONE, 2012, 7, e45696.	1.1	34
192	Epithelial-Stromal Interactions in Human Breast Cancer: Effects on Adhesion, Plasma Membrane Fluidity and Migration Speed and Directness. PLoS ONE, 2012, 7, e50804.	1.1	83
193	Daily On-Line Set-Up Correction in 3D-Conformal Radiotherapy: Is It Feasible?. Tumori, 2012, 98, 441-444.	0.6	26
194	Janus-faced liposomes enhance antimicrobial innate immune response in <i>Mycobacterium tuberculosis</i> infection. Proceedings of the National Academy of Sciences of the United States of America, 2012, 109, E1360-8.	3.3	60
195	Volumetric Modulated Arc Therapy with Simultaneous Integrated Boost for Locally Advanced Rectal Cancer. Clinical Oncology, 2012, 24, 261-268.	0.6	31
196	Celiac disease and pregnancy outcome: anti-transglutaminase antibodies effects on placental and endometrial functions. Journal of Reproductive Immunology, 2012, 94, 28.	0.8	0
197	PE_PGRS30 is required for the full virulence of Mycobacterium tuberculosis. Cellular Microbiology, 2012, 14, 356-367.	1.1	100
198	Novel fluorescent security marker. Part I: morphological and optical properties of 2-amino-6-ethoxy-4-[4-(4-morpholinyl)phenyl]-3,5-pyridinedicarbonitrile nanoparticles. Journal of Nanoparticle Research, 2012, 14, 1.	0.8	8

#	Article	IF	CITATIONS
199	Daily on-line set-up correction in 3D-conformal radiotherapy: is it feasible?. Tumori, 2012, 98, 441-4.	0.6	11
200	The R1306W Type 2B Natural Mutation of Von Willebrand Factor Dramatically Enhances the Multimer Sensitivity to Shear Stress. Blood, 2012, 120, 3306-3306.	0.6	0
201	Effects of Mechanical Forces on the Cellular Dynamics. Biophysical Journal, 2011, 100, 304a.	0.2	0
202	Nanocavities trapped along fibrin fibers allow the diffusion of thrombolytic drugs. Applied Physics Letters, 2011, 99, 223701.	1.5	3
203	Docosahexaenoic acid reverts resistance to UV-induced apoptosis in human keratinocytes: involvement of COX-2 and HuR. Journal of Nutritional Biochemistry, 2011, 22, 874-885.	1.9	31
204	Controlled self assembly of collagen nanoparticle. Journal of Nanoparticle Research, 2011, 13, 6141-6147.	0.8	42
205	The Thermal Structural Transition of α-Crystallin Inhibits the Heat Induced Self-Aggregation. PLoS ONE, 2011, 6, e18906.	1.1	15
206	Heat Stress Causes Spatially-Distinct Membrane Re-Modelling in K562 Leukemia Cells. PLoS ONE, 2011, 6, e21182.	1.1	59
207	Mechanical properties of zona pellucida hardening. European Biophysics Journal, 2010, 39, 987-992.	1.2	62
208	Compartmentalization of the redox environment in PC-12 neuronal cells. European Biophysics Journal, 2010, 39, 993-999.	1.2	11
209	Clâ^' and Fâ^' anions regulate the architecture of protofibrils in fibrin gel. European Biophysics Journal, 2010, 39, 1001-1006.	1.2	11
210	Ristocetin-induced self-aggregation of von Willebrand factor. European Biophysics Journal, 2010, 39, 1597-1603.	1.2	30
211	Intervillous circulation in intra-uterine growth restriction. Correlation to fetal well being. Placenta, 2010, 31, 1051-1056.	0.7	35
212	Natural lysophospholipids reduce Mycobacterium tuberculosis â€induced cytotoxicity and induce antiâ€mycobacterial activity by a phagolysosome maturationâ€dependent mechanism in A549 type II alveolar epithelial cells. Immunology, 2010, 129, 125-132.	2.0	30
213	Thiol Redox Transitions in Cell Signaling: a Lesson from N-Acetylcysteine. Scientific World Journal, The, 2010, 10, 1192-1202.	0.8	77
214	Mammalian life-span determinant p66 ^{shcA} mediates obesity-induced insulin resistance. Proceedings of the National Academy of Sciences of the United States of America, 2010, 107, 13420-13425.	3.3	96
215	Reactive Oxygen Species as Essential Mediators of Cell Adhesion and Migration. Biophysical Journal, 2010, 98, 576a.	0.2	2
216	Fibrin Gel Ultrastructure. Biophysical Journal, 2010, 98, 59a.	0.2	0

#	Article	IF	CITATIONS
217	Fluctuations and the Rate-Limiting Step of Peptide-Induced Membrane Leakage. Biophysical Journal, 2010, 99, 1791-1800.	0.2	49
218	Protective Role of 17-β-Estradiol in LDL Amyloidogenesis. Biophysical Journal, 2010, 98, 484a.	0.2	0
219	Estradiol Binding Prevents ApoB-100 Misfolding in Electronegative LDL(â^'). Biochemistry, 2010, 49, 7297-7302.	1.2	18
220	Nutrient withdrawal rescues growth factor-deprived cells from mTOR-dependent damage. Aging, 2010, 2, 487-503.	1.4	33
221	Evidence of elastic to plastic transition in the zona pellucida of oocytes using atomic force spectroscopy. Applied Physics Letters, 2009, 94, .	1.5	41
222	CpG oligodeoxynucleotides promote phospholipase D dependent phagolysosome maturation and intracellular mycobacterial killing in M. tuberculosis infected type II alveolar epithelial cells. Cellular Immunology, 2009, 259, 1-4.	1.4	6
223	Investigation of the spatial distribution of glutathione redox-balance in live cells by using Fluorescence Ratio Imaging Microscopy. Biosensors and Bioelectronics, 2009, 25, 682-687.	5.3	25
224	On The Mechanisms Regulating Alpha-crystallin Activity. Biophysical Journal, 2009, 96, 90a.	0.2	0
225	Generation in Human Plasma of Misfolded, Aggregation-Prone Electronegative Low Density Lipoprotein. Biophysical Journal, 2009, 97, 628-635.	0.2	23
226	Physical Properties of the Zona Pellucida. Biophysical Journal, 2009, 96, 337a.	0.2	1
227	Growth, viability, adhesion potential, and fibronectin expression in fibroblasts cultured on zirconia or feldspatic ceramics <i>in vitro</i> . Journal of Biomedical Materials Research - Part A, 2008, 86A, 959-968.	2.1	28
228	470: Gadolinium-enhanced MRI mapping of placental perfusion in normal and IUGR pregnancies. American Journal of Obstetrics and Gynecology, 2008, 199, S140.	0.7	1
229	Role of the life span determinant P66shcA in ethanol-induced liver damage. Laboratory Investigation, 2008, 88, 750-760.	1.7	69
230	N-acetyl-l-cysteine fosters inactivation and transfer to endolysosomes of c-Src. Free Radical Biology and Medicine, 2008, 45, 1566-1572.	1.3	33
231	Detection of microviscosity by using uncalibrated atomic force microscopy cantilevers. Applied Physics Letters, 2008, 93, 124102.	1.5	28
232	High-Resolution Imaging of Redox Signaling in Live Cells Through an Oxidation-Sensitive Yellow Fluorescent Protein. Science Signaling, 2008, 1, pl3.	1.6	48
233	Low density lipoprotein misfolding and amyloidogenesis. FASEB Journal, 2008, 22, 2350-2356.	0.2	48
234	Modifications in solvent clusters embedded along the fibers of a cellulose polymer network cause paper degradation. Physical Review E, 2008, 77, 041801.	0.8	28

#	Article	IF	CITATIONS
235	Globular structure of human ovulatory cervical mucus. FASEB Journal, 2007, 21, 3872-3876.	0.2	74
236	Sphingosine 1-phosphate promotes antigen processing and presentation to CD4+ T cells in Mycobacterium tuberculosis-infected monocytes. Biochemical and Biophysical Research Communications, 2007, 361, 687-693.	1.0	11
237	Low Density Lipoprotein Aged in Plasma Forms Clusters Resembling Subendothelial Droplets: Aggregation via Surface Sites. Biophysical Journal, 2006, 90, 4239-4247.	0.2	34
238	Fluid viscosity determination by means of uncalibrated atomic force microscopy cantilevers. Applied Physics Letters, 2006, 88, 194102.	1.5	42
239	Modifications of the Mesoscopic Structure of Cellulose in Paper Degradation. Physical Review Letters, 2006, 97, 238001.	2.9	27
240	CpG oligodeoxynucleotides induce Ca2+-dependent phospholipase D activity leading to phagolysosome maturation and intracellular mycobacterial growth inhibition in monocytes. Biochemical and Biophysical Research Communications, 2006, 347, 963-969.	1.0	10
241	Lysophosphatidic acid enhances antimycobacterial activity both in vitro and ex vivo. Clinical Immunology, 2006, 121, 23-28.	1.4	22
242	Simultaneous static and dynamic light scattering approach to the characterization of the different fibrin gel structures occurring by changing chloride concentration. Applied Physics Letters, 2005, 86, 183901.	1.5	24
243	Particle Size Distribution in DMPC Vesicles Solutions Undergoing Different Sonication Times. Biophysical Journal, 2005, 88, 3545-3550.	0.2	128
244	Small- and wide-angle elastic light scattering study of fibrin structure. Journal of Applied Crystallography, 2003, 36, 636-641.	1.9	36
245	Protofibrils within fibrin fibres are packed together in a regular array. Thrombosis and Haemostasis, 2003, 89, 632-636.	1.8	24
246	Protofibrils within fibrin fibres are packed together in a regular array. Thrombosis and Haemostasis, 2003, 89, 632-6.	1.8	9
247	Structure of fibrin gels studied by elastic light scattering techniques: Dependence of fractal dimension, gel crossover length, fiber diameter, and fiber density on monomer concentration. Physical Review E, 2002, 66, 011913.	0.8	57
248	Aggregation kinetics and structure of cryoimmunoglobulins clusters. Physica A: Statistical Mechanics and Its Applications, 2002, 304, 211-219.	1.2	4
249	Growth kinetics and structure of fibrin gels. Physical Review E, 2001, 63, 031401.	0.8	54
250	On the dynamics of semiflexible fibrin gels. Macromolecular Symposia, 2000, 162, 263-274.	0.4	3
251	Time-resolved dynamic light scattering as a method to monitor compaction during protein folding. Macromolecular Symposia, 2000, 162, 205-220.	0.4	2

252 Light scattering characterization of fibrin gels. , 2000, , .

#	Article	IF	CITATIONS
253	Internal dynamics of semiflexibles fibrin networks. , 1999, , .		Ο
254	Dynamic light scattering study of fine semiflexible fibrin networks. Biophysical Chemistry, 1997, 67, 287-292.	1.5	14
255	Self-similarity properties of alpha-crystallin supramolecular aggregates. Biophysical Journal, 1995, 69, 2720-2727.	0.2	28
256	Relaxation dynamic measurements in fibrin networks. , 1993, , .		0
257	Birefringence and scattering in highly oriented artificial Kerr media. Optics Letters, 1991, 16, 120.	1.7	9
258	Field-induced polarization modulation in shaped-microparticle suspensions. Journal of the Optical Society of America B: Optical Physics, 1991, 8, 2370.	0.9	6
259	Nondegenerate two-wave mixing in shaped microparticle suspensions. , 1991, , .		0
260	Non-linear optics in artificial Kerr materials. Materials Science and Engineering B: Solid-State Materials for Advanced Technology, 1991, 9, 509-515.	1.7	0
261	Polarization-resolved beam combination in liquid suspensions of shaped microparticles. Physical Review A, 1991, 44, 7580-7596.	1.0	10
262	Optical phase conjugation through translational and rotational diffusive rearrangements of liquid-dispersed microparticles. Physical Review A, 1990, 41, 2882-2885.	1.0	12
263	Third-order nonlinearity enhancement in an artificial Kerr medium through bulk intrinsic birefringence. Optics Letters, 1989, 14, 239.	1.7	11
264	Polarization-resolved optical phase conjugation in an artificial anisotropic Kerr medium. Optics Letters, 1989, 14, 1356.	1.7	5